NON-BREAKING AND BREAKING WAVE LOADS
ON A COOLING WATER OUTFALL

by

G.R. Mogridge* and W.W. Jamieson**

ABSTRACT

Cooling water from a power generating station in Eastern Canada is pumped to an outfall and distributed into the ocean through discharge ports in the sidewalls of a diffuser cap. The cap is essentially a shell-type structure consisting of a submerged circular cylinder 26.5 ft in diameter and 14 ft high. It is located in 25 ft of water at low water level and 54 ft at high water level. Horizontal forces, vertical forces and overturning moments exerted by waves on a 1:36 scale model of the diffuser cap were measured with and without cooling water discharging from the outfall. Tests were run with regular and irregular waves producing both non-breaking and breaking wave loads on the diffuser cap.

The overturning moments measured on the diffuser cap were up to 150 percent greater than those on a solid submerged cylinder sealed to the seabed. Unlike sealed cylinders, all of the wave loads measured on the relatively open structure reached maximum values at approximately the same time. The largest wave loads were measured on the diffuser structure when it was subjected to spilling breakers at low water level. For a given wave height, the spilling breakers caused wave loads up to 100 percent greater than those due to non-breaking waves.

INTRODUCTION

A power generating station, located on the east coast of Canada, disposes of cooling water through a 12 ft diameter tunnel a distance of approximately 300 ft offshore, where it rises vertically to a diffuser structure which distributes the water through a number of discharge ports into the Bay of Fundy. The large arrows, in the schematic representation of the cooling water outfall in Fig. 1(a), indicate the flow direction of the warm water through the tunnel, into the diffuser cap and out of the discharge ports. The diffuser cap is a shell-type structure consisting basically of a submerged concrete circular cylinder with a solid top, an open bottom and a number of 5.5 ft square openings in the sidewalls. It is 26.5 ft in diameter, 14 ft high and is held in place by rock anchors. The bottom of the cap does not make a perfect seal with the seabed because of numerous gaps between the bottom of the structure and the seabed around its circumference. The cooling water outfall is located in a water depth of 25 ft at low water level (LWL), 39 ft at mean water level (MWL) and 54 ft at high water level (HWL). Since waves up to 50 ft high are expected at this location, the structure is exposed to breaking waves. The five arrows radiating outward from the diffuser cap in Fig. 1(b) show the direction of cooling water discharge in

*Associate and **Assistant Research Officers, Hydraulics Laboratory, Division of Mechanical Engineering, National Research Council of Canada, Ottawa, Ontario, Canada, K1A 0R6.

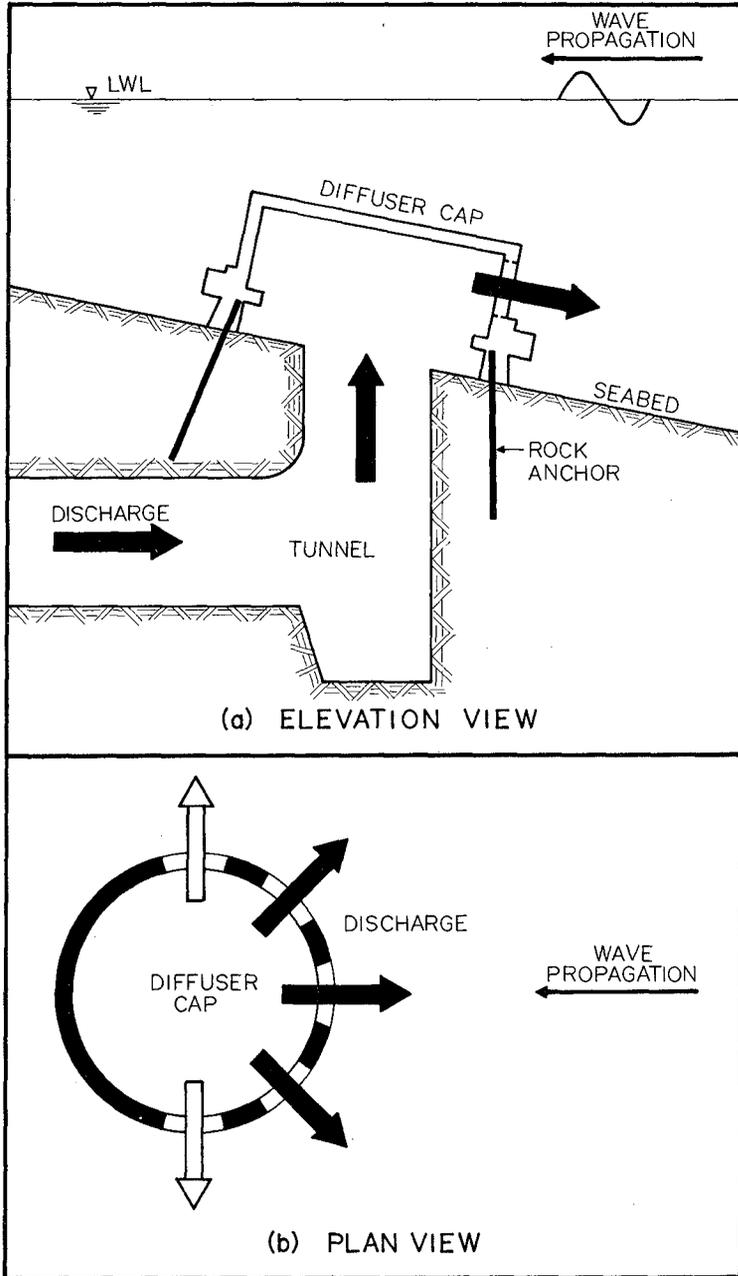(a) ELEVATION VIEW

(b) PLAN VIEW

FIG.1 COOLING WATER OUTFALL

relation to the direction of wave propagation. The three shaded arrows indicate the present requirements of the power generating station, which call for 3 discharge ports (N=3) and a cooling water discharge Q of 300,000 gpm (US). In the near future, the cooling water outfall will be required to handle a discharge of 450,000 gpm (US) with five discharge ports (N=5) in operation as indicated by the five arrows in Fig. 1(b). After being damaged during a storm in February 1976, the anchoring system had to be redesigned to secure the diffuser cap to the seabed. The loads exerted by ocean waves and cooling water discharge were required to permit a safe design of the structure and its rock anchors.

        Various methods, which use linear wave theory and neglect viscous effects, are available for predicting wave loads on large submerged structures resting on the seabed. For example, Garrison and Chow (6), and Hogben and Standing (10) have published linear numerical diffraction theories which use a source distribution over the immersed surface of a structure for the prediction of wave loads. For ease of computation, these methods have been simplified by Black (1), Garrison and Stacey (8), Fenton (4) and Isaacson (11). Gran (9) has presented an analytical method which does not satisfy all the boundary conditions but provides an approximate solution at minimum cost. Black, Mei and Bray (2) have presented a semi-analytical method using variational calculus while Yue, Chen and Mei (14) have proposed a method that they refer to as a hybrid element method which combines the use of variational principles and finite element techniques. All of these methods assume that structures, which sit on a flat bottom, are both solid and sealed to the seabed. For structures raised slightly above the seabed, both experimental and theoretical results have been presented by Gran (9) for cylinders, and by Chakrabarti and Naftzger (3) and Garrison and Snider (7) for hemispherical shells. To the authors' knowledge, no information is available in the literature concerning the calculation of wave loads on a relatively large shell-type structure such as the diffuser cap, which is not only raised above the seabed but has large openings in the sidewalls. The prediction of the maximum design loads on the diffuser cap is further complicated by the existence of irregular waves, cooling water discharge and critically steep waves that result in spilling breakers in the vicinity of the outfall during storm conditions.

        Since reliable theoretical methods were not available for predicting the wave loading on such a complex structure, it was necessary to perform model tests. The loading due to non-breaking and breaking waves in regular and irregular wave trains, and the effects of cooling water discharge were measured using a 1:36 Froude model. A digital computer was used for the acquisition, processing, plotting and storage of the experimental data.

EXPERIMENTAL METHOD

        The photograph in Fig. 2 shows the 1:36 plexiglass scale model of the diffuser cap which was positioned in the centre of a 12 ft wide wave flume. A semiconductor strain gauge force dynamometer was used to measure the forces and overturning moments on the model. The sign convention (Fig.3) was chosen such that the horizontal force $F_x(t)$ is positive in the direction of wave propagation, the vertical force $F_z(t)$ is positive in the upward direction and the overturning moment $M_y(t)$ is positive in the counter-clockwise direction. The force dynamometer had an overall
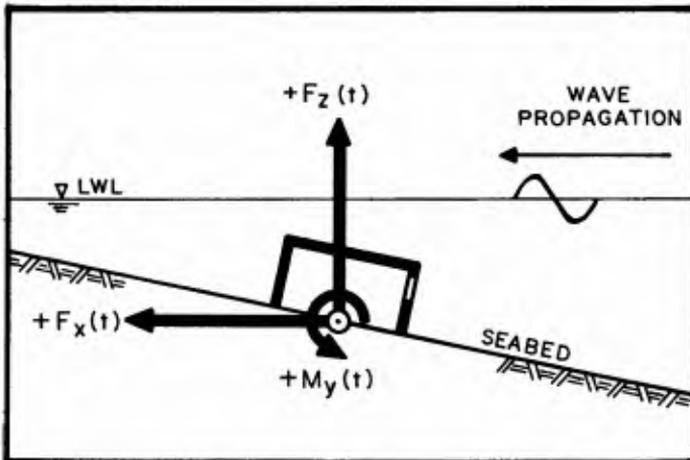
FIG. 2 MODEL OF DIFFUSER CAP

FIG.3 SIGN CONVENTION

accuracy of within plus or minus three percent. It was mounted in a cavity
in the floor of the wave flume below a steel base plate which was flush with
the bottom. The diffuser cap was connected rigidly to the force dyna-
mometer by four aluminum rods which passed freely through holes in the
steel base plate. The discharge pipe, that was used in the model to
simulate the prototype cooling water tunnel, did not touch or interfere
with the operation of the force dynamometer. The exit of the model
discharge pipe can be seen in Fig. 2 through the discharge port in the
front of the diffuser cap. The natural frequency of vibration of the
total measuring system with the model mounted was approximately 75 Hz
when submerged in water, and therefore was sufficiently high to elimin-
ate resonance problems.

In Fig. 4, the elevation and plan views of the wave flume show
the experimental setup. Beach slopes, modelled from the prototype con-
tours, were 1:50 offshore of the diffuser cap, 1:5 in the immediate vic-
inity of the cap and 1:8 onshore. Simulation of the cooling water dis-
charge to the model was accomplished by a 300 gpm (US) pump and measured
by a calibrated orifice meter. Water was pumped out of a reservoir at
the end of the flume through a 2 in. diameter pipe to the diffuser cap
and returned via two 3 in. diameter pipes under the floor of the flume
from the area of the wave generator. Wave profiles were measured by two
capacitance wave probes located as shown in Fig. 4.

Acquisition of data for forces, moments and wave profiles was
accomplished using a digital computer. Force, moment and wave profile
data were sampled at a rate of 100 data points per second for an inter-
val of 8 sec. For irregular waves this rate was decreased to 20 data
points per second to give total record lengths of 50 sec. The data was
analysed and the results were automatically plotted and printed immedi-
ately following each test.

EXPERIMENTAL RESULTS

Non-Breaking Waves

To determine the effects of wave period T and water depth d on
wave loading, the diffuser cap was subjected to regular non-breaking
waves for various wave periods and wave heights at LWL, MWL and HWL.
Fig. 5 shows typical test results for time series plots of wave loads
and water surface elevations $\eta(t)$ measured at the diffuser cap and
upwave of the cap. It may be observed that the phasing of the wave
loads and water surface elevation are such that all the loads, $F_x(t)$,
$F_z(t)$ and $M_y(t)$, reach maximum positive values near the time of still
water level (SWL). Throughout the testing program, the experimental
results indicated that the maximum positive magnitudes of the wave
loads were always greater than the maximum negative values. Thus, only
the magnitudes of the maximum positive loads will be considered in this
paper. Fig. 6 shows the experimental measurements for the maximum values
of horizontal force F_x, vertical force F_z and overturning moment M_y plot-
ted against wave height H measured at the diffuser cap, for wave periods
between 6 and 16 sec. There is only a small variation of wave loads
with wave period, although the magnitudes of the wave loads tend to be
largest at 10 and 12 sec. A larger variation in wave loading results
for different depths of submergence of the diffuser cap as shown in Fig.
7. The largest forces and moments were measured on the diffuser cap
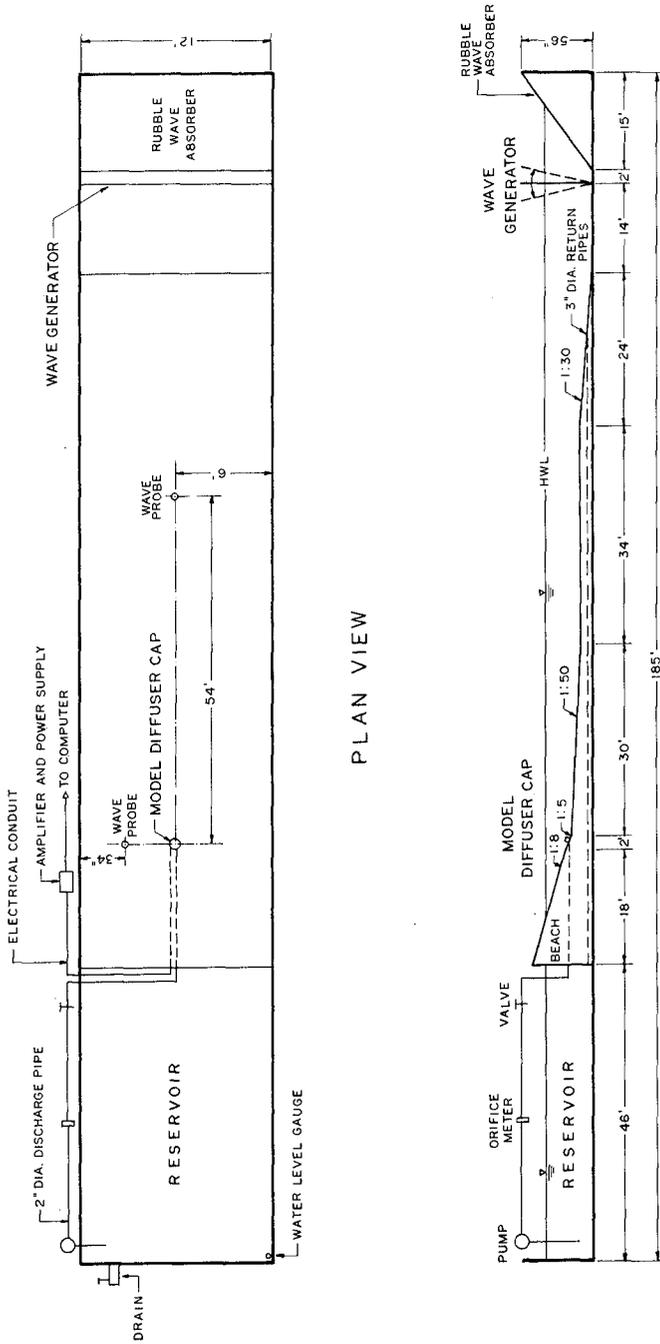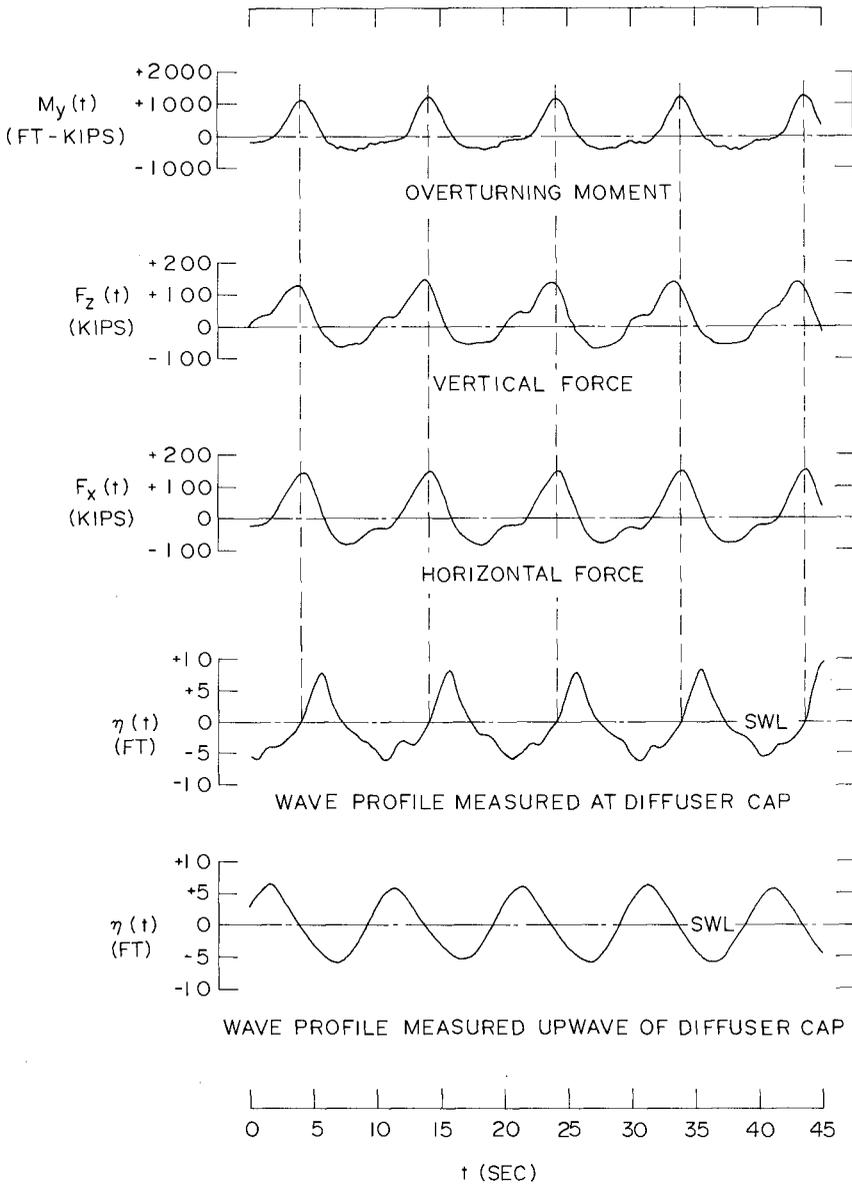when it was located in the shallowest water depth of 25 ft (LWL).

PLAN VIEW

ELEVATION VIEW

FIG. 4 ELEVATION AND PLAN VIEWS OF WAVE FLUME
        SHOWING EXPERIMENTAL SETUP

FIG.5 TYPICAL TEST RESULTS
NON-BREAKING REGULAR WAVES
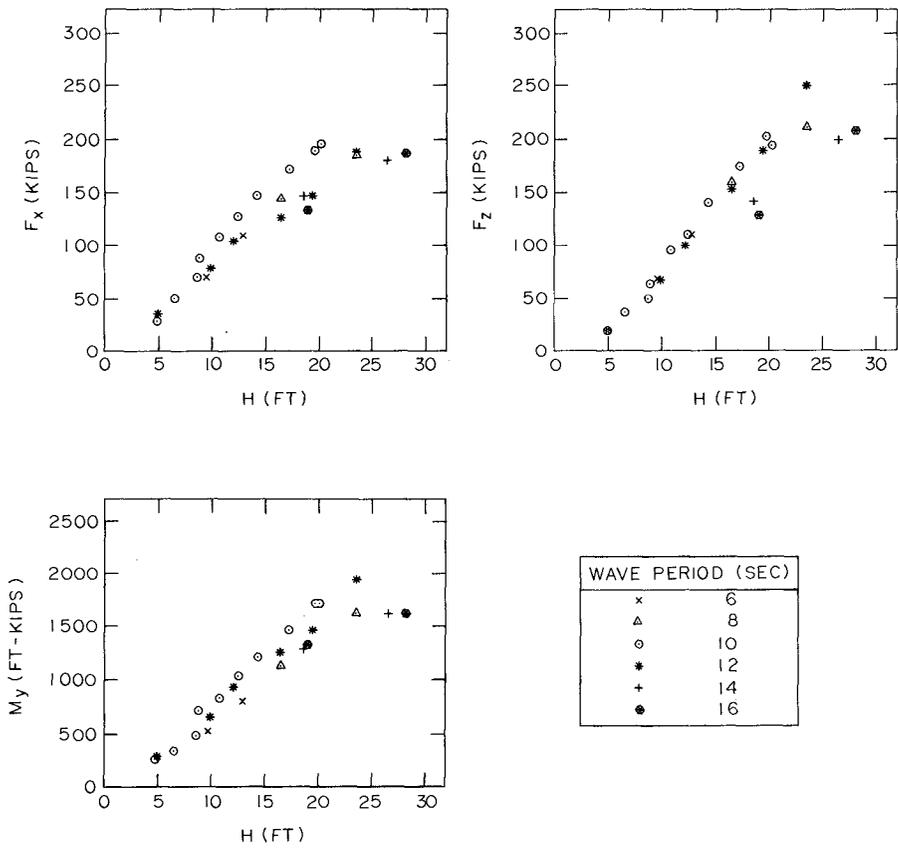(N = 3, Q = 0, d = 25 FT, T = 10 SEC)

FIG. 6   VARIATION OF WAVE LOAD WITH WAVE PERIOD
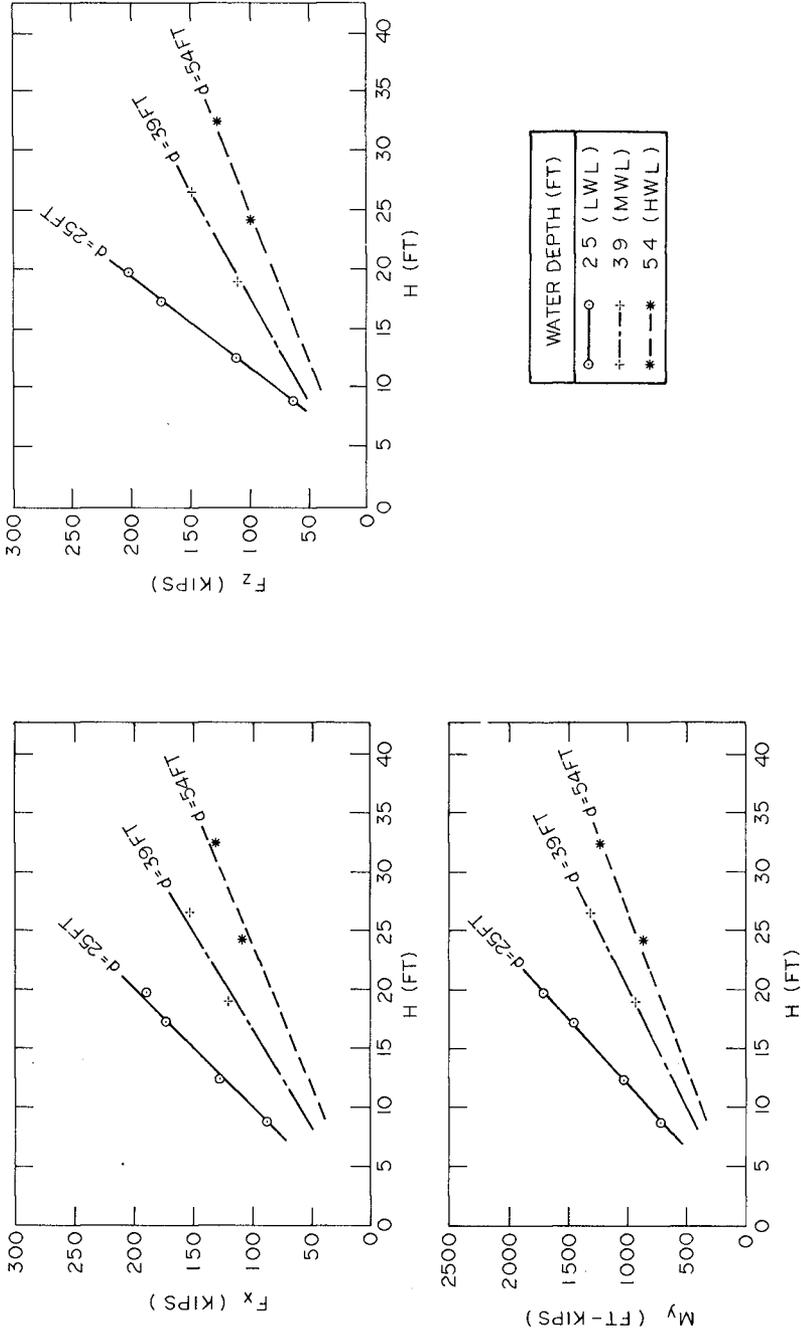NON - BREAKING REGULAR WAVES
(N=3 , Q=O , d = 25 FT)

FIG.7 VARIATION OF WAVE LOAD WITH WATER DEPTH
NON-BREAKING REGULAR WAVES
(N = 3 , Q = 0 , T = 10 SEC)

A rigorous theoretical method for the prediction of non-breaking wave loads on a relatively open structure such as the diffuser cap does not presently exist. It may be of interest, however, to demonstrate some of the similarities and differences in wave loading between a ported submerged structure, such as the diffuser cap, and a solid submerged structure which is sealed to the seabed. Fig. 8 shows results for a wave period of 12 sec and a water depth of 25 ft for non-breaking regular waves. The wave loading shown for the sealed submerged cylinder, 26.5 ft in diameter and 14 ft high, was calculated using the linear numerical diffraction theory of Hogben and Standing (10).

The horizontal wave forces measured on the diffuser cap are quite similar in magnitude to those on the sealed submerged cylinder. However, it should be mentioned that for some tests, the horizontal forces on the diffuser cap vary as much as plus or minus 25 percent from those on the sealed cylinder. For both structures, F_x occurs approximately at the time of SWL which is indicative of inertial predominant horizontal forces.

The overturning moments on the diffuser cap are significantly larger than those on the sealed submerged cylinder calculated by the diffraction theory and are in fact up to 150 percent larger for some tests. For both the diffuser cap and the sealed cylinder, M_y occurs approximately at SWL.

The vertical forces measured on the diffuser cap are up to 75 percent smaller than those calculated for the sealed submerged cylinder (Fig. 8). The maximum vertical forces for the two cases not only vary significantly in magnitude, but also occur at different times with respect to the wave profile. The maximum uplift forces on the diffuser cap occur approximately at SWL, while those on the sealed cylinder occur near the wave trough. Similar phasing results were obtained experimentally by filling the diffuser cap with styrofoam, which caused the maximum vertical force to occur approximately at the trough; however, when the styrofoam was removed, the phasing reverted back to F_z occurring near the time of SWL. Thus, all the wave loads on the diffuser cap reach maximum values at the same time, resulting in a far more critical loading situation than for the sealed structure where F_z is out of phase with respect to F_x and M_y. The difference in phasing for the diffuser cap is due to the existence of the discharge ports in the offshore side of the cap. Calculations have indicated that if the same magnitude of pressure that exists on the offshore side of the sealed submerged cylinder is allowed to enter through the discharge ports into the diffuser cap, and contributions due to drag are included, a reasonable estimate of the total uplift force on the diffuser cap is possible and it is found to occur approximately at SWL as measured by experiment.

Gran (9) has shown that a gap underneath a solid cylinder causes similar variations in loading. That is, the gap tends to reduce the magnitude of F_z, increase M_y and have little effect on F_x. Garrison and Snider (7), and Chakrabarti and Naftzger (3) have also demonstrated that a substantial reduction in vertical force occurs when a hemispherical shell is held slightly above the ocean bottom, while the horizontal forces remain approximately the same. The analysis of Chakrabarti and Naftzger (3) shows that the pressure inside may be assumed to be uniform for small values of ka and can be approximated by the average pressure at the bottom of the corresponding sealed structure. The force on the raised structure can then be calculated by subtracting this pressure times the
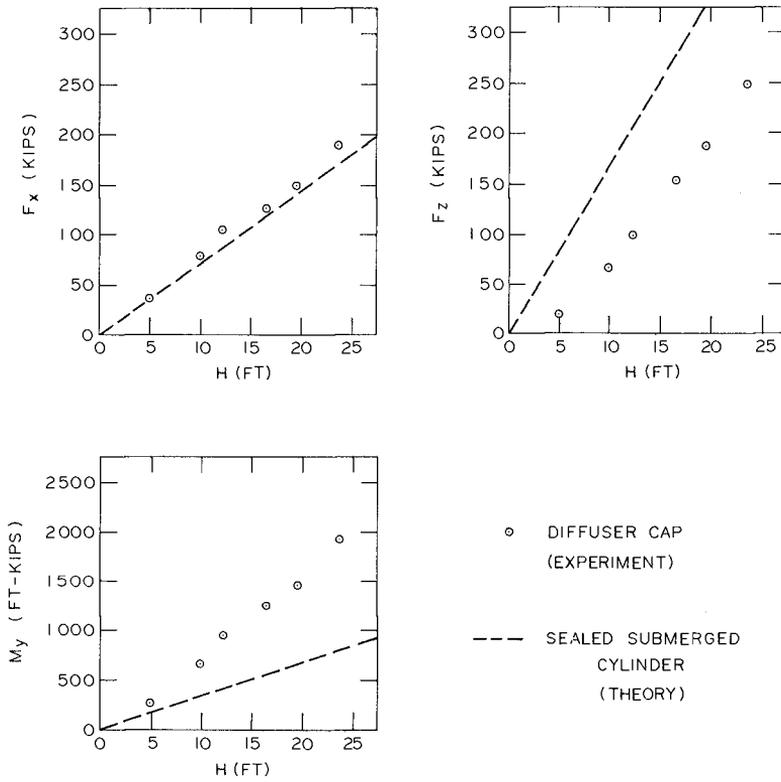
FIG.8 COMPARISON OF EXPERIMENTAL AND THEORETICAL RESULTS
NON-BREAKING REGULAR WAVES
(N = 3, Q = 0, d = 25 FT, T = 12 SEC)

area of the base from the force on the sealed structure. The same assumption of uniform pressure inside the structure cannot be made for the diffuser cap, since it has ports on one side causing an asymmetrical pressure distribution. The ports also cause the maximum vertical forces to occur approximately at SWL, whereas for the structures studied by the above authors, maximum values occurred near the trough.

For vertical circular cylinders projecting through the water surface, Mogridge and Jamieson (12) have indicated that there may be some viscous drag effects in the horizontal forces for ka less than 2.8, which for the diffuser cap diameter of 26.5 ft would be for periods greater than 10 sec. However, for the diffuser cap, the horizontal forces are almost entirely inertial, while the vertical forces appear to be due to the combined effects of inertia and drag. In order to substantiate this statement, the F_x and F_z data in Fig. 8 has been replotted in Fig. 9 on a logarithmic scale. Since inertial force is directly proportional to wave height, inertial force can be represented by a straight line with a slope of 1:1. In this plot, the solid line with a slope of 1:1 is fitted through the horizontal force data. A reasonably good fit confirms the existence of inertial predominant horizontal forces. The vertical force data in Fig. 9 lies on a slope greater than 1:1 and thus the force is not solely inertial but is due to the combined contributions of inertial force, drag force and possibly non-linear wave effects. The slope depends on the proportion of drag to inertial force and whether the drag coefficient is constant or a function of wave height.

Breaking Waves

Breaking wave forces were also measured on the diffuser cap. The regular non-breaking wave heights were increased until relatively steep waves were generated at the wave board. The combination of these steep waves and the gentle bottom slope of 1:50 created spilling breakers in the vicinity of the diffuser cap. The magnitudes of the vertical forces due to spilling breakers were always maximum in the positive or upward direction. Occasionally, a plunging wave would break on the diffuser cap; however, this still did not cause the negative vertical forces to be larger than the positive values, possibly because even at LWL there was enough water above the diffuser cap to cushion the force of the breakers.

Non-breaking and breaking wave load data are plotted in Fig. 10 for N=3 and N=5. For a given wave height, spilling breakers often produce wave loads much larger than those caused by non-breaking waves. The data for the most extreme breaking wave conditions indicate wave loads as much as 100 percent greater than for non-breaking waves.

The breaking waves produce much more scatter in the wave load data than the non-breaking waves. The breaking mechanism apparently affects the period of the waves. Although the periods of the individual waves measured near the wave generator were all approximately 12 sec, at the diffuser cap a range of wave periods were measured. This variation in wave period at the structure probably accounts for some of the scatter of the data. However, most of the scatter is probably due to the variation in the degree of breaking at the structure. Spillage at the crest rapidly reduces the wave height, but does not significantly alter the fluid accelerations or pressures on the structure. Although not

—— INERTIAL FORCE ➡ SLOPE = 1 : 1 (F ∝ H)
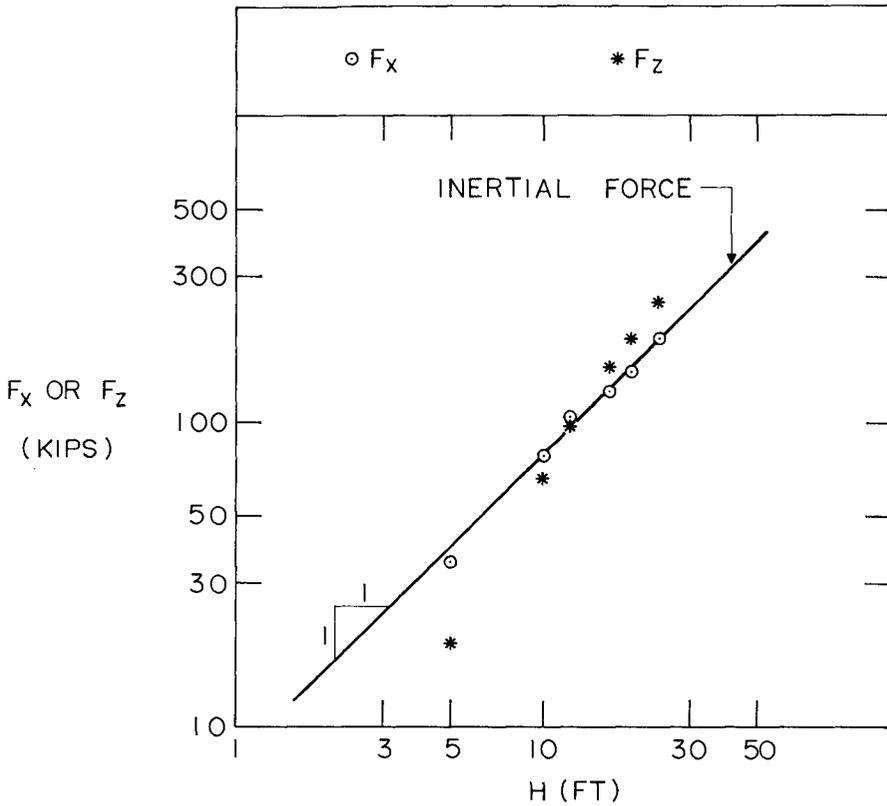
INERTIAL FORCE + DRAG FORCE ➡ SLOPE > 1 : 1

FIG.9 LOGARITHMIC PLOT OF F_X AND F_Z
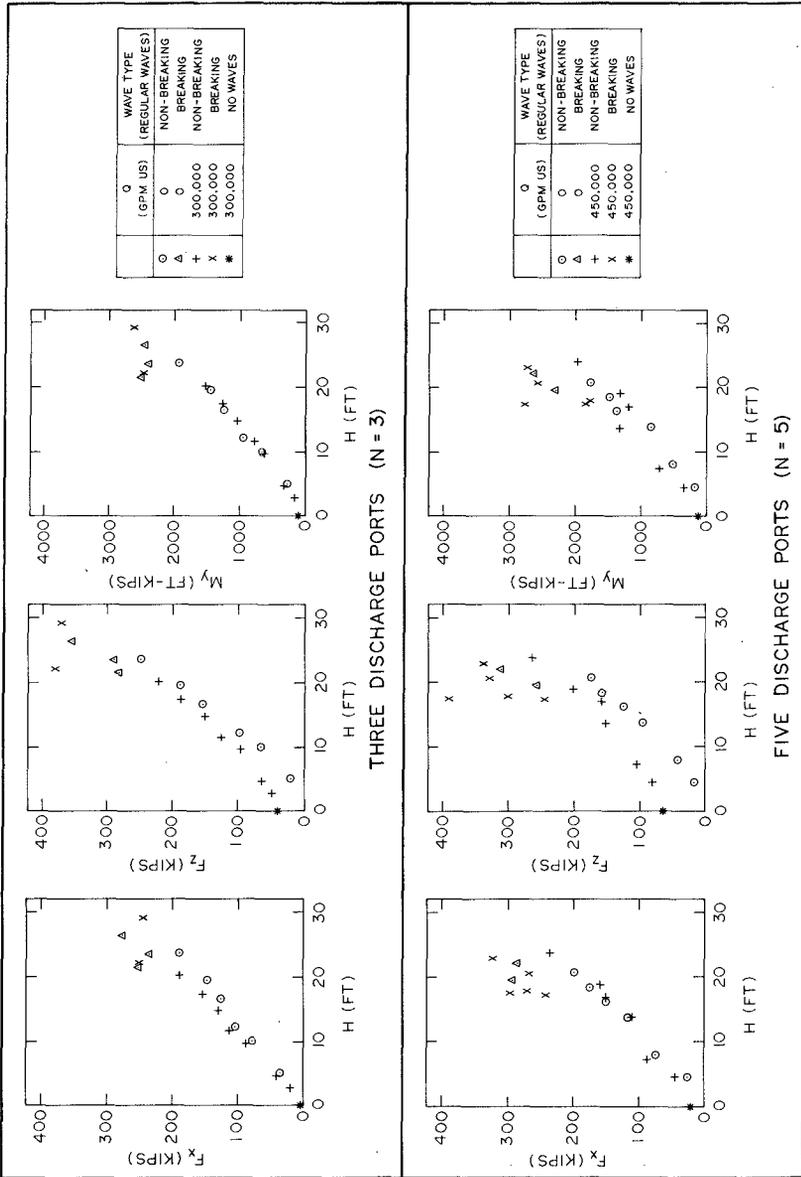NON-BREAKING REGULAR WAVES
(N = 3, Q = 0, d = 25 FT, T = 12 SEC)

FIG. IO WAVE FORCES AND OVERTURNING MOMENTS

(d = 25 FT , T = 12 SEC)

shown here, wave loads can be plotted against instantaneous wave slope
at the time of maximum loadings as in Mogridge and Jamieson (13) and
correlations are somewhat better than plotting against wave height.
        The maximum loads due to breaking waves generally occur near the
time of SWL as for non-breaking waves, but there is enough of a phase
shift in some tests to indicate that higher velocities cause significant
increases in viscous drag forces.

Cooling Water Discharge

        The effect of cooling water discharge on the wave loading is shown
in Fig. 10. The upper plots show the results with a discharge of 300,000
gpm (US) while the lower plots are for 450,000 gpm(US). F_x and M_y show
minimal differences in loading due to cooling water discharge for both
non-breaking and breaking wave conditions. However, F_z does increase
considerably due to discharge, particularly for low wave heights. For
breaking waves, the increase in F_z due to discharge is not as well de-
fined as for non-breaking waves because of the considerable scatter in
the data caused by the spilling breakers.

Irregular Waves

        The time series plot of the water surface elevation for the storm,
which damaged the diffuser cap in February 1976, is shown in Fig. 11.
This 20 minute prototype wave record, measured in relatively deep water,
was reproduced directly in the wave flume at the wave board. That is, a
Fourier analysis decomposed the wave record into sinusoidal components
described by amplitude and phase angle for each frequency. Predetermined
transfer functions, compensating for water depth and wave generator char-
acteristics, were applied to each frequency component to give voltage
amplitudes for generation of the required wave amplitudes at the wave
board. Then, by means of an inverse Fourier transform, a voltage time
series was obtained and used as input to the wave machine for the simula-
tion of the prototype wave profile in the flume. Using this method of
irregular wave generation, actual wave records can be reproduced with
correct phasing between frequency components, which is important when
grouping is present in the wave records. Further details are available
in the report by Funke and Mansard (5).
        A comparison of the prototype spectrum and the model spectrum mea-
sured 54 ft upwave of the diffuser cap at HWL, is shown in Fig. 12. The
significant wave heights in the prototype and the model were 18.3 ft and
18.7 ft respectively, while the peak wave period was 13.4 sec in both
spectra. This was one of the better fits between the model and prototype
spectra because at HWL the water was sufficiently deep in the wave flume
to minimize wave shoaling between the wave board and the wave probe.
        The irregular waves, generated in the wave flume, produced non-
breaking and breaking waves at the diffuser cap. As with regular waves,
the wave loads reached maximum values at approximately the time of SWL
and the largest wave loadings were measured at LWL. The analysis of the
irregular wave data was treated on a wave-to-wave basis; that is, the
largest wave loads and corresponding zero up-crossing wave heights were
selected over the entire wave height range, disregarding wave period.
Fig. 13 shows a comparison of the wave loading results due to the
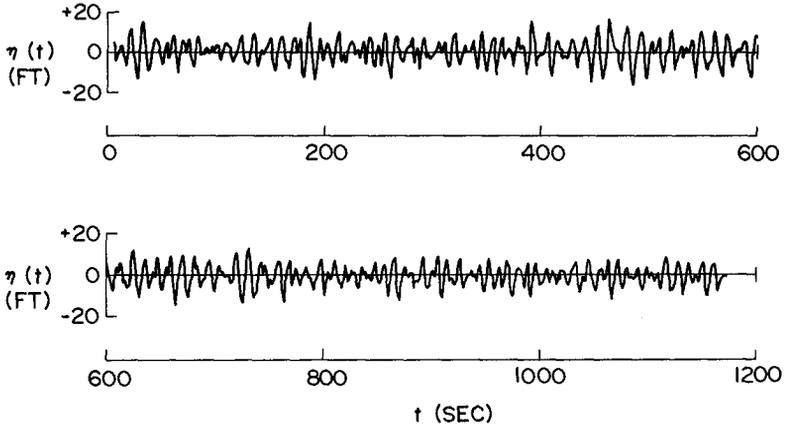February 1976 storm, and the 10 and 12 sec regular waves. More scatter
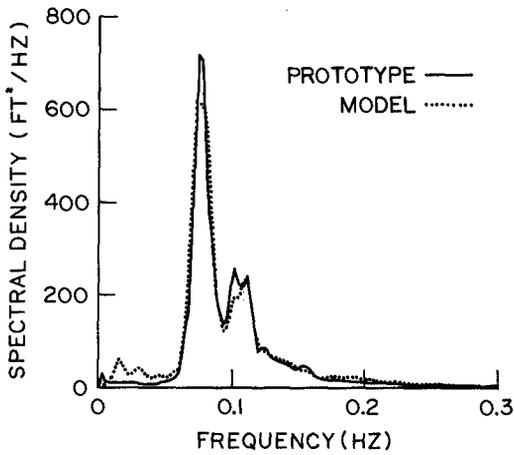
FIG.11 PROTOTYPE WAVE PROFILE
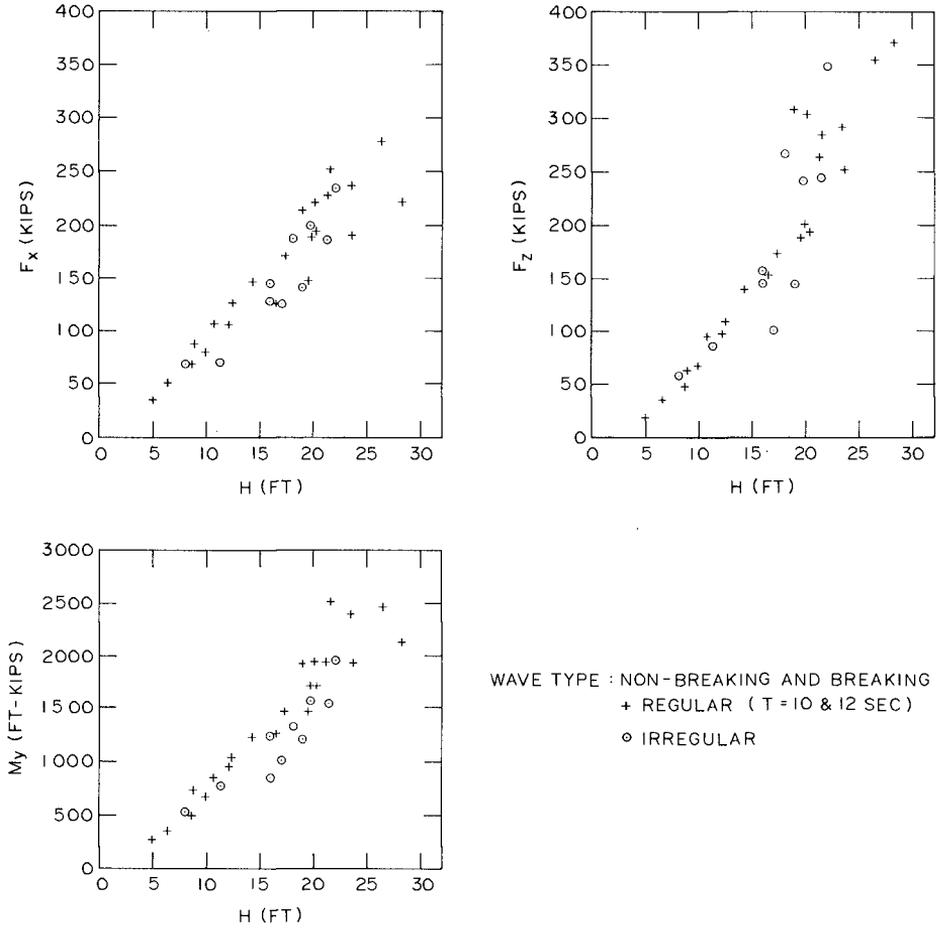(FEBRUARY 2,1976,1500HR)

FIG.12 WAVE SPECTRA

FIG.13 COMPARISON OF RESULTS FOR REGULAR
AND IRREGULAR WAVES
(N = 3 , Q = O , d = 25 FT)

results for the irregular waves because there is a much wider frequency
range present than just 10 and 12 sec, and also because there is some
breaking of the higher frequency waves even at low wave heights. Based
on the limited number of tests analysed, using only one irregular wave
record which consisted essentially of non-grouped waves, it appears that
irregular wave loads are no more severe than regular wave loads. Neglig-
ible differences were also observed (13) between irregular and regular
wave loadings when cooling water discharges of 300,000 gpm (US) and
450,000 gpm (US) were used. It should be emphasized that the irregular
wave record used for these tests, produced the maximum possible wave
heights and steepnesses at the diffuser cap because of the depth limita-
tion. Therefore, it is most unlikely that any other irregular wave re-
cord would produce wave loads any higher. This does not mean that in
general, wave load tests need not be conducted using irregular waves.
On the contrary, it is possible that where wave heights are not limited
by water depth, interaction of wave frequencies may produce groups of
very high steep waves creating large structural loads. In addition, if
it is anticipated that structural fatigue may be a problem, load distri-
bution functions should be measured using irregular waves.

CONCLUSIONS

Horizontal forces, vertical forces and overturning moments on the
diffuser cap of a cooling water outfall have been determined. Existing
theoretical methods cannot be used to predict the loading on such an
open submerged structure as the diffuser cap which is subjected not only
to the combined loading of non-breaking waves and cooling water discharge,
but also the extreme loadings imposed by breaking waves. A model testing
program has resulted in the following conclusions:
1. A large variation in wave period causes only a small variation in
    wave loading. A larger variation in loading results for different
    depths of submergence of the diffuser cap. The largest forces and
    overturning moments, for a given wave height, occurred at low water
    level for 10 and 12 sec waves.
2. It cannot be assumed that the magnitude of the maximum wave loads
    on a shell-type structure raised above the bottom with ports in the
    sidewalls will be similar to those on a sealed structure. For
    example, the wave loads on the diffuser cap were such that, compared
    to a sealed submerged cylinder, the horizontal forces were generally
    within plus or minus 25 percent, the vertical forces were up to 75
    percent smaller and the overturning moments were up to 150 percent
    larger.
3. All of the wave loads on a ported structure, similar to the diffuser
    cap, reach maximum values at about the same time. This results in a
    far more critical loading situation than for a sealed structure where
    the vertical force is approximately 90 degrees out of phase with res-
    pect to the horizontal force and overturning moment.
4. For a given wave height, spilling breakers on the diffuser cap caused
    loads up to 100 percent greater than those due to non-breaking waves.
    For both the non-breaking and breaking waves, the magnitude of the
    vertical force was always maximum in the upward direction.
5. Tests performed with simultaneous wave loading and cooling water dis-
    charge indicated that for low wave heights, the discharge through the
    diffuser structure could increase the uplift forces considerably;

however, for high waves and particularly for spilling breakers, the
discharge did not significantly affect the magnitude of the wave
loads.
6. Based on the limited number of tests using a non-grouped irregular
    wave train, the magnitudes of the maximum irregular wave loads on
    the diffuser cap were no more severe than the regular wave loads.
    This conclusion does not necessarily apply in general to other sit-
    uations where such factors as wave grouping or fatigue stresses may
    be important.

ACKNOWLEDGEMENTS

REFERENCES

1. Black, J.L., "Wave Forces on Vertical Axisymmetric Bodies", Journal
    of Fluid Mechanics, Vol. 67, Part 2, 1975, pp. 369-376.
2. Black, J.L., C.C. Mei and M.C.G. Bray, "Radiation and Scattering
    of Water Waves by Rigid Bodies", Journal of Fluid Mechanics, Vol. 46,
    Part 1, 1971, pp. 151-164.
3. Chakrabarti, S.K. and R.A. Naftzger, "Wave Interaction with a
    Submerged Open-Bottom Structure", Eighth Annual Offshore Technology
    Conference, Houston, Paper No. OTC 2534, May, 1976, pp. 109-123.
4. Fenton, J.D., "Wave Forces on Vertical Bodies of Revolution",
    Journal of Fluid Mechanics, Vol. 85, Part 2, 1978, pp. 241-255.
5. Funke, E.R. and E.P.D. Mansard, "Reproduction of Prototype Random
    Wave Trains in a Laboratory Flume", Hydraulics Laboratory, National
    Research Council of Canada, Ottawa, Laboratory Technical Report
    No. LTR-HY-64, December, 1978.
6. Garrison, C.J. and P.Y. Chow, "Wave Forces on Submerged Bodies",
    Proc. ASCE, Vol. 98, No. WW3, August, 1972, pp. 375-392.
7. Garrison, C.J. and R.H. Snider, "Wave Forces on Large Submerged
    Tanks", Coastal and Ocean Engineering Division, Texas A&M Univer-
    sity, Report No. 117-COE, January, 1970, 83 pp.
8. Garrison, C.J. and R. Stacey, "Wave Loads on North Sea Gravity
    Platforms: A Comparison of Theory and Experiment", Ninth Annual
    Offshore Technology Conference, Houston, Paper No. OTC 2794, May,
    1977, pp. 513-524.
9. Gran, S., "Wave Forces on Submerged Cylinders", Fifth Annual
    Offshore Technology Conference, Houston, Paper No. OTC 1817,
    April-May, 1973, pp. 801-812.
10. Hogben, N. and R.G. Standing, "Wave Loads on Large Bodies",
    International Symposium on the Dynamics of Marine Vehicles and
    Structures in Waves, edited by R.E.D. Bishop and W.G. Price,
    Mechanical Engineering Publications Limited, London, 1975, pp.
    258-277.
11. Isaacson, M. de St. Q., "Vertical Cylinders of Arbitrary Section in
    Waves", Proc. ASCE, Vol. 104, No. WW4, August, 1978, pp. 309-324.
12. Mogridge, G.R. and W.W. Jamieson, "Wave Loads on Large Circular
    Cylinders: A Design Method", Division of Mechanical Engineering,
    National Research Council of Canada, Ottawa, Mechanical Engineering

Report No. MH-111, December, 1976, 40 pp.

13.   Mogridge, G.R. and W.W. Jamieson, "Wave Loads on a Cooling Water Outfall, Coleson Cove, N.B.", Hydraulics Laboratory, National Research Council of Canada, Ottawa, Laboratory Technical Report No. LTR-HY-63, November, 1977, 101 pp.

14.   Yue, D.K.P., H.S. Chen and C.C. Mei, "A Hybrid Element Method for Diffraction of Water Waves by Three-Dimensional Bodies", International Journal for Numerical Methods in Engineering, Vol. 12, 1978, pp. 245-266.

NOTATION

a	Radius of hemisphere or cylinder
d	Water depth
$F_x(t)$	Horizontal force as a function of time
F_x	Maximum value of $F_x(t)$
$F_z(t)$	Vertical force as a function of time
F_z	Maximum value of $F_z(t)$
H	Wave height at diffuser cap
k	Wave number, $k = 2\pi/L$
L	Wave length
$M_y(t)$	Overturning moment as a function of time
M_y	Maximum value of $M_y(t)$
N	Number of discharge ports in diffuser cap
Q	Discharge through diffuser cap
T	Wave period
t	Time
$\eta(t)$	Water surface elevation as a function of time
π	3.141592...